Non Intrusive Reduced Basis method (NIRB)

The Two-grids method

Elise Grosjean [1]
In collaboration with: Yvon Maday [1], Nora Aïssiouene[1]

[1] Laboratoire Jacques-Louis Lions
Sorbonne Université

GTT 2020

Industrial context $\rightarrow$ black box solver (BB)

Non intrusive reduced basis method useful for:

- Optimization parameters fitting
- High fidelity real-time simulations

Goal: Solve for several parameters the same parameter dependent problem and reduce the computational costs

Several methods:

- Finite Element method
- Extension to Finite Volume method

A model problem

$$
\begin{cases}
-\operatorname{div}(A(\mu)\nabla u) = f \text{ in } \Omega, & \text{(1a)}\\
u = 0 \text{ on } \partial\Omega, & \text{(1b)}
\end{cases}
$$

- $u(\mathbf{x};\mu)$: Unknowns (u_h on the fine mesh $\mathcal{T}_h$, u_H on the coarse mesh $\mathcal{T}_H$).
- $\mu \in \mathbb{R}$: Variable parameter

$f \in L^2(\Omega)$,
$A : \Omega \times \mathbb{R} \to \mathcal{M}_d(\mathbb{R})$ is measurable, bounded, uniformly elliptic, and $A(\mathbf{x})$ is symmetric for a.e. $\mathbf{x} \in \Omega$.

Scheme NIRB OFFLINE/ONLINE

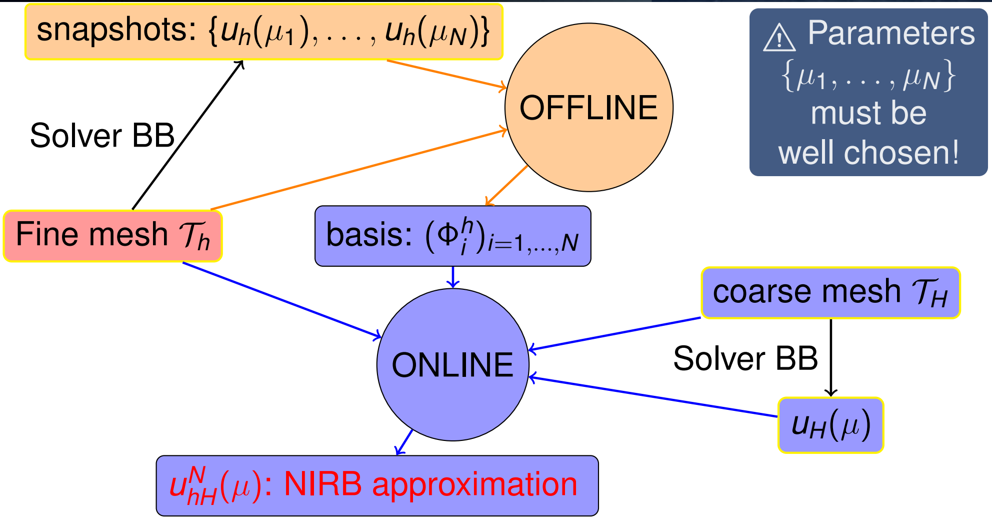

How to choose the parameters

- Greedy algorithm
- Observing the decay of eigenvalues with an SVD

Kolmogorov n-width must be small [1] $\mathcal{M}_h = \{u_h(\mu) \in V_h | \ \mu \in \mathcal{P}\}$ is a subset of a Banach space V_h.
The Kolmogorov n-width of $\mathcal{M}_h$ in V_h is

$$d_n(\mathcal{M}_h, V_h) = \inf_{Y_n}\{ \sup_{x\in\mathcal{M}_h} (\inf_{y\in Y_n} \|x-y\|_{V_h}); \mathrm{Y_n \text{ is a } n\text{-dimensional subspace of }} V_h\}. \qquad (2)$$

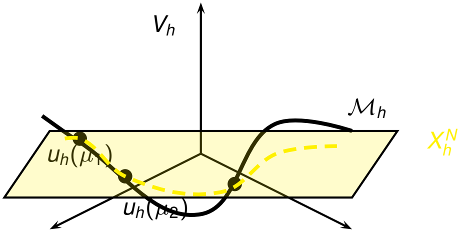

[1] A. Buffa, Y. Maday, A.T. Patera, C. Prudhomme, and G. Turinici, *A Priori convergence of the greedy algorithm for the parameterized reduced basis.* 2010

Projection Orthogonal Decomposition (POD)

Objective: Choose a basis which represents the most likely realizations!

Observing the decay of eigenvalues with an SVD.

$$\max_{\Phi \in L^2} \frac{\overline{|u, \Phi|^2}}{\|\Phi\|^2} = \frac{\overline{|u, \Psi|^2}}{\|\Psi\|^2}. \tag{3}$$

This problem is equivalent to finding the biggest eigenvalue to the following equation

$$C\Psi = \lambda\Psi, \tag{4}$$

where $C_{i,j} = \int_\Omega u_i \cdot u_j$.

NIRB algorithm: Offline stage

1. Compute the approximations $\{u_h(\mu_i)\}_{i\in\{1,\dots N\}}$.

2. Two cases can be considered:
   - A greedy algorithm with a Gram-Schmidt procedure $\rightarrow L^2$ orthonormalization.
   - (optional) Complemented by the following problem: Find $\Phi \in X_h^N$, and $\lambda \in \mathbb{R}$ such that

$$\forall v \in X_h^N, \int_\Omega \nabla\Phi \cdot \nabla v = \lambda \int_\Omega \Phi \cdot v, \tag{5}$$

$\rightarrow L^2(\Omega)$ and $H^1(\Omega)$ orthogonalization.

$$X_h^N = Vect\{u_h(\mu_1), \dots, u_h(\mu_N)\}$$

NIRB algorithm: Online stage

3. Solve problem on the coarse mesh $\mathcal{T}_H$ where $H >> h$ with μ.
4. $\alpha_i^H = \int_\Omega I^h(u_H(\mu)) \cdot \Phi_i^h$ and output: $u_{Hh}^N = \sum_{i=1}^{N} \alpha_i^H \Phi_i^h$.
5. (Optional) Post-Treatment (PT)

$$\left\| u(x;\mu) - \sum_{k=1}^{N} (u_H(\mu), \phi_k^h)\, \phi_k^h \right\|_{H^1} \leq \overbrace{\epsilon}^{T_1} + \underbrace{C_1 h}_{T_2} + \overbrace{C_2 H^2}^{T_3} \sim Ch$$

if $H^2 \sim h$

where C_1, C_2 are constants independent of h and H.[2]

[2] Rachida Chakir, Yvon Maday. *A two-grid finite-element/reduced basis scheme for the approximation of the solution of parameter dependent PDE.* 2009

Some recalls for T_2 and T_3 with FEM

Cea's Lemma

$$\|u - u_h\|_{H^1} \leq C \inf_{v_h \in V_h} \|u - v_h\| \leq Ch\|u\|_{H^2}$$

Aubin-Nitsche's Lemma

$$\|u - u_h\|_{L^2} \leq Ch\|u - u_h\|_{H^1} .$$

What if we only have access to the nodes?

Consider $\mathbb{P}_1$ finite elements

$a(u_h, v_h) = (f, v_h).$

Solution u_h $\quad\quad \tilde{u}_h = \tilde{I}_h(u_h)$

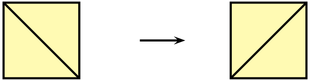

$$\left\|u - \tilde{u}_h\right\|_{H^1} \leq Ch.$$ [3]

[3] Susanne C. Brenner, L. Ridgway Scott. *The Mathematical Theory of Finite Element Methods*, 2008.

The rectification method

$(u_H^i, \Phi_j) \rightarrow (u_h^i, \Phi_j)$

$$(A_i)_k = (u_H(\mu_k), \Phi_i)_{L^2}, \forall k = 1, \cdots, Ntrain \tag{6}$$

$$(B_i)_k = (u_h(\mu_k), \Phi_i)_{L^2}, \forall k = 1, \cdots, Ntrain \tag{7}$$

$$D = (A_1, \cdots, A_N) \in \mathbb{R}^{Ntrain \times N} \tag{8}$$

$$\tag{9}$$

$$T_i = (D^T D + \lambda I_N)^{-1} D^T B_i, \ \forall i = 1, \cdots, N. \tag{10}$$

$$u_{Hh}^N(\mu) = \sum_{i,j=1}^{N} T_{ij}(u_H(\mu), \Phi_j)\Phi_i \tag{11}$$

Results with FE

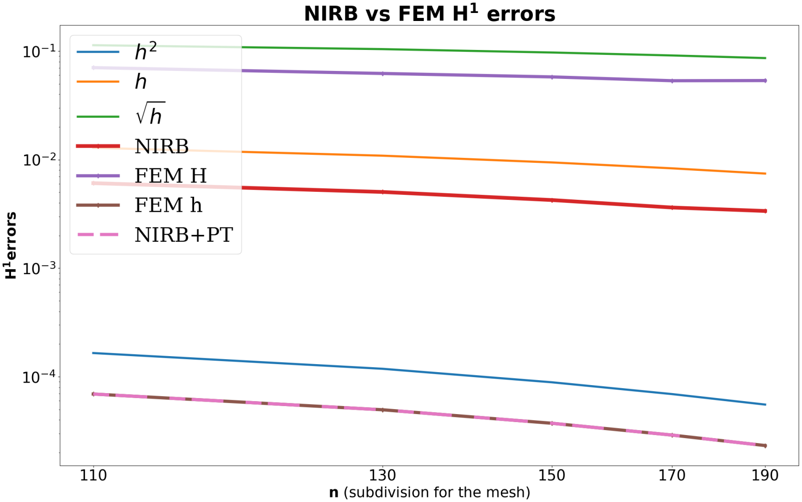

Polytopal mesh for FV

$$X_{\mathcal{D},0} = \{v = ((v_K)_{K\in\mathcal{M}}, (v_\sigma)_{\sigma\in\mathcal{F}}) : v_K \in \mathbb{R}, v_\sigma \in \mathbb{R}, v_\sigma = 0 \text{ if } \sigma \in \mathcal{F}_{ext}\}.$$

Goal:
Extend FE estimate
to FV solver

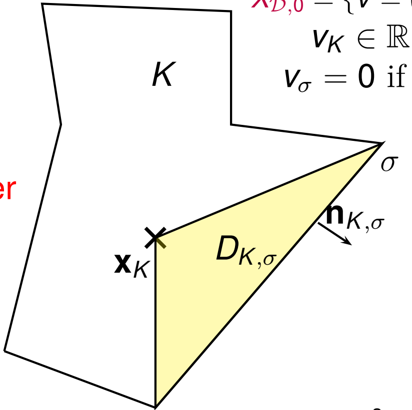

Figure: A cell K of a polytopal mesh [3]

[3] J. Droniou, R. Eymard, T. Gallouët, C. Guichard, R. Herbin. *The gradient discretisation method.* 2018

Hybrid Mimetic Mixed (HMM) scheme

Stokes Formula:

$$-\sum_{\sigma\in\mathcal{F}_K}\int_\sigma \nabla u(\mathbf{x})\cdot\mathbf{n}_{K,\sigma}\, d_\gamma(\mathbf{x}) = \int_K f(\mathbf{x})d\mathbf{x}. \quad (12)$$

Flux balance:

$$\sum_{\sigma\in\mathcal{F}_K} F_{K,\sigma} = \int_K f(\mathbf{x})\, d(\mathbf{x}). \quad (13)$$

Flux conservativity:

$$F_{K,\sigma} + F_{L,\sigma} = 0. \quad (14)$$

Gradient Discret scheme

$$\begin{cases} -\operatorname{div}(A(\mu)\nabla u) = f \text{ in } \Omega, & (15a) \\ u = 0 \text{ on } \partial\Omega, & (15b) \end{cases}$$

Variational Gradient Scheme [4]

Find $u_{\mathcal{D}} \in X_{\mathcal{D},0}$ such that, $\forall v_{\mathcal{D}} \in X_{\mathcal{D},0}$,

$$\int_{\Omega} A(\mu)\nabla_{\mathcal{D}} u_{\mathcal{D}} \cdot \nabla_{\mathcal{D}} v_{\mathcal{D}} = \int_{\Omega} f\, \Pi_{\mathcal{D}} v_{\mathcal{D}}. \quad (16)$$

[4] J. Droniou, R. Eymard, T. Gallouët, C. Guichard, R. Herbin. *The gradient discretisation method.* 2018

Hybrid Mimetic Mixed (HMM) scheme: Operators

1. $\Pi_{\mathcal{D}} : X_{\mathcal{D},0} \to L^2(\Omega)$:

   $\forall v \in X_{\mathcal{D},0}, \forall K \in \mathcal{M},\ \Pi_{\mathcal{D}} v(\mathbf{x}) = v_K \text{ on } K.$

2. $\nabla_{\mathcal{D}} : X_{\mathcal{D},0} \to L^2(\Omega)^d$:

   $\forall v \in X_{\mathcal{D},0}, \forall K \in \mathcal{M}, \forall \sigma \in \mathcal{F},$

   $\nabla_{\mathcal{D}} v(\mathbf{x}) = \nabla_K v + S \text{ on } D_{K,\sigma}$, where S ensures stability and

   $\nabla_K v = \frac{1}{|K|} \sum_{\sigma \in \mathcal{F}_K} |\sigma| v_\sigma \mathbf{n}_{K,\sigma}$.

A norm on $X_{\mathcal{D},0}$: $\|\cdot\|_{\mathcal{D}} = \|\nabla_{\mathcal{D}} \cdot\|_{L^2(\Omega)^2}$.

Error estimate

H^1 error estimate

Goal: $\left\| u(\mu) - u^N_{Hh}(\mu) \right\|_{\mathcal{D}} \leq Ch$

$$\left\| u(\mu) - u^N_{Hh}(\mu) \right\|_{\mathcal{D}} \leq T_1 + T_2 + T_3$$

$$T_1 = \left\| u(\mu) - \Pi^h_{\mathcal{D}} u_h(\mu) \right\|_{\mathcal{D}},$$

$$T_2 = \left\| \Pi^h_{\mathcal{D}} u_h(\mu) - u^N_{hh}(\mu) \right\|_{\mathcal{D}},$$

$$T_3 = \left\| u^N_{hh}(\mu) - u^N_{Hh}(\mu) \right\|_{\mathcal{D}},$$

where $u^N_{hh}(\mu) = \sum_{i=1}^{N} \alpha^h_i(\mu) \Pi^h_{\mathcal{D}} \Phi^h_i$.

Error estimate

1. From classical result on FV :

$$T_1 = \left\| u(\mu) - \Pi_{\mathcal{D}}^h u_h(\mu) \right\|_{\mathcal{D}} \leq C_1 h. \qquad (17)$$

2. Result from Kolmogorov n-width [5]:

$$T_2 = \left\| \Pi_{\mathcal{D}}^h u_h(\mu) - \sum_{i=1}^{N} \alpha_i^h(\mu) \Pi_{\mathcal{D}}^h \Phi_i^h \right\|_{\mathcal{D}} \leq \epsilon.$$

3. From a super-convergence property [6],

$$\left| \int_{\Omega} (u(\mu) - \Pi_{\mathcal{D}}^H u_H(\mu)) \cdot \Pi_{\mathcal{D}}^h \Phi_i^h \right| \leq C_2 H^2, \forall \Phi_i^h \in X_h^N, \qquad (18)$$

We deduce $T_3 \leq C_2 H^2$.

---

[5] Rachida Chakir, Yvon Maday. *A two-grid finite-element/reduced basis scheme for the approximation of the solution of parameter dependent PDE.* 2009

[6] J. Droniou, N. Nataraj, *Improved L2 estimate for gradient schemes, and super-convergence of HMM and TPFA finite volume methods*, 2016.

Some details on item 3

Super-convergence

$$\left|\int_\Omega (u(\mu) - \Pi_{\mathcal{D}}^H u_H(\mu)) \cdot \Pi_{\mathcal{D}}^h \Phi_i^h\right| \leq C_2 H^2, \text{ for all } \Phi_i^h \in X_h^N. \quad (19)$$

$\Pi_0^H : \mathcal{C}(\Omega) \to L^\infty(\Omega)$:

$$\Pi_0^H \Phi = \Phi(\mathbf{x}_K), \text{ on } K\ \forall K \in \mathcal{M}_H, \forall \Phi \in \mathcal{C}(\Omega). \quad (20)$$

$\Pi_1^H : \mathcal{C}(\Omega) \to \mathbb{R}$ (affine projection $\Pi_1^H(u) = Q^2 u(\mathbf{x}, \mu)$, see Taylor polynomial of order 2 of $u(\mu)$ averaged over B_K):

$$Q^2 u(\mathbf{x}, \mu) = \int_B [u(\mathbf{x_K}; \mu) + \nabla u(\mathbf{y}; \mu)(\mathbf{x} - \mathbf{x}_K)] \Psi(\mathbf{y})\, d\mathbf{y}. \quad (21)$$

such that $\Pi_1^H(u(\mathbf{x}_K, \mu))_{|K} = u(\mathbf{x}_K)$

Some details on item 3

$$\left|\int_\Omega (u(\mu) - \Pi_{\mathcal{D}}^H u_H(\mu)) \cdot \Pi_{\mathcal{D}}^h \Phi_i^h\right| \leq T_4 + T_5 + T_6, \qquad (22)$$

where

$$T_4 = |(u - \Pi_1 u, \Phi)|,\ T_5 = |(\Pi_1 u - \Pi_0 u, \Phi)|,\ T_6 = |(\Pi_0 u - \Pi_{\mathcal{D}} u_H, \Phi)|.$$

Some details on item 3

- Bramble-Hilbert's Lemma:

$$\left\|u(\mu)-\Pi_1^H(u(\mu))\right\|_{L^2(\Omega)} \leq \tilde{C}_2 H^2 \left\|u(\mu)\right\|_{H^2(\Omega)}, \tag{23}$$

- $$\left\|u(\mu)-\Pi_0^H u(\mu)\right\|_{L^2(\Omega)} \leq \tilde{C}_1 H \left\|u(\mu)\right\|_{H^2(\Omega)}. \tag{24}$$

- Average property:

$$\int_K \Pi_1^H(u(\mu))(\mathbf{x})\cdot\zeta(\mathbf{x})d\mathbf{x} = \int_K \Pi_0^H u(\mathbf{x})\cdot\zeta(\mathbf{x})d\mathbf{x}, \forall K \in \mathcal{M}_H, \forall \zeta \text{ such that } \zeta_{|K} \in \mathbb{P}_0. \tag{25}$$

- $$\left\|\Pi_{\mathcal{D}} u_H(\mu)-\Pi_0^H(u(\mu))\right\|_{L^2(\Omega)} \leq CH^2. \tag{26}$$

One application: 2D Wind turbine

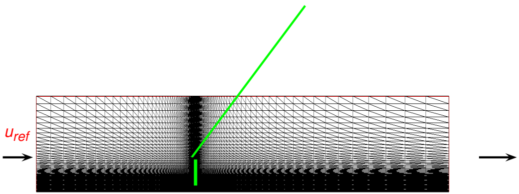

Figure 1: Mesh for one wind turbine

- 2D mesh with 6500 cells, thinner around the wind turbine.
- Characteristic length D: 126m, corresponds to the rotor diameter.
- Hub height: 95.6m.
- Wind turbine rotor is represented in the movement equation by adding a source term.
- Boundary Condition: u_{ref} at the inlet.
- Initial Condition: u_{ref} set in the domain.

u_{ref}: Variable parameter

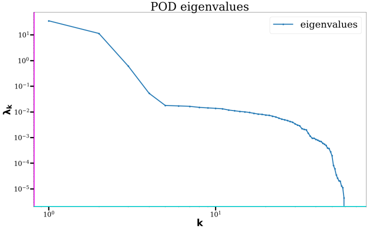

Figure 2: Decrease of the eigenvalues of the POD

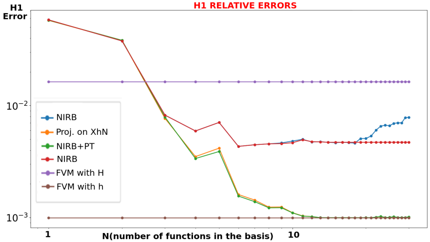

Figure 3: H^1 errors of the velocity on the interest area

- For $k = 3$, $I(k) = \frac{\sum_{j=1}^{k} \lambda_j}{\sum_{j=1}^{N} \lambda_j} \simeq 1$.
- The error of NIRB increases slightly after $N = 15$ (Figure 3).
- The relative error of $\left\| u_{h/10} - u_{Hh}^N \right\|_{H^1}$ is between the one given by $\left\| u_{h/10} - u_h \right\|_{H^1}$ and the one with u_H (Figure 3).

Wind turbines in 3D

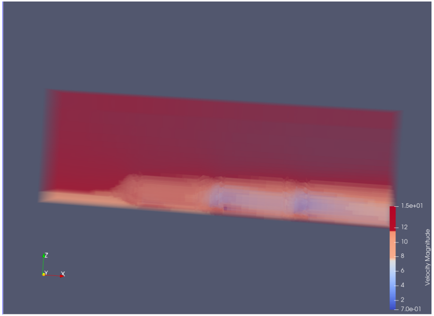

Wind canal with less opacity

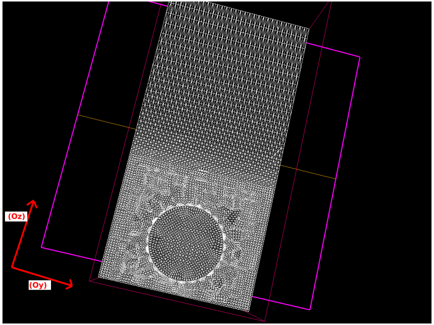

One wind turbine mesh ($\mathcal{N} \sim 500\,000$)

Results for 3D application

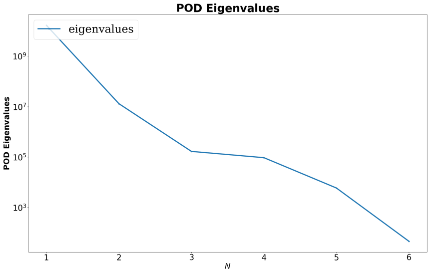

Eigenvalues

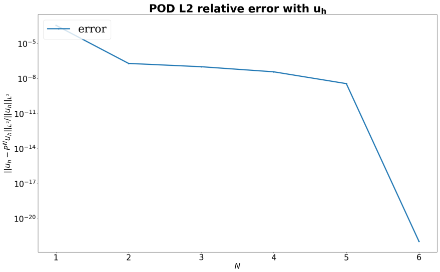

Relative L^2 error

Conclusion and Perspectives:

1. Extend the error estimates from FE to FV solver and retrieve the classical errors.
2. Numerical results with FV solver in accordance with expectations in 2D and 3D.

Perspectives:

- Extend 3D wind turbines to offshore wind farm,
- Use different applications,
- Generalize to other FV schemes.

Thank you for your attention!

Elise Grosjean